The impact of measurement scale on the univariate statistics of K, Th, and U in the Earth crust

David Baratoux[1], Makhoudia Fall[2], Pierre-Yves Meslin[3], Mark Jessell[4], Olivier Vanderheaghe[5], Jean-François Moyen[6], Papa Moussa Ndiaye[2], Kwame Boamah[7], Lenka Baratoux[8], and Anne-Sylvie André-Mayer[9]

[1]Université Félix Houphouët-Boigny
[2]University Cheikh Anta Diop
[3]IRAP-OMP
[4]University of Western Australia
[5]Géosciences Environnement Toulouse, University of Toulouse
[6]Univ. St-Etienne
[7]Geological Survey Department of Ghana
[8]Institut de Recherche pour le Développement
[9]Université de Lorraine

November 22, 2022

Abstract

The univariate statistics of Potassium (K), Thorium (Th) and Uranium (U) concentrations, in the Earth's oceanic and continental crust are examined by different techniques. The frequency distributions of the concentrations of these elements in the oceanic crust are derived from a global catalog of mid-ocean ridge basalts (MORB). Their frequency distributions of concentrations in the continental crust are illustrated by the North Pilbara Craton, and the West Africa Craton. For these two cratons, the distributions of K, Th and U derived from geochemical analyses of several thousand whole rock samples differ significantly from those derived from airborne radiometric surveys. The distributions from airborne surveys tends to be more symmetric with smaller standard deviations than the right-skewed distributions inferred from whole rock geochemical analyses. Hypothetic causes of these differences include (i) bias in rock sampling or in airborne surveys, (ii) the differences in the chemistry of superficial material, and (iii) the differences in scales of measurements. The scale factor, viewed as consequence of the central limit theorem applied to K, Th and U concentrations, appears to account for most of the observed differences in the distributions of K, Th and U. It suggests that the three scales of auto-correlation of K, Th and U concentrations are of the same order of magnitude as the resolution of the airborne radiometric surveys (50 – 200 m) and concentrations of K, Th, U are therefore generally heterogenous at smaller scales.
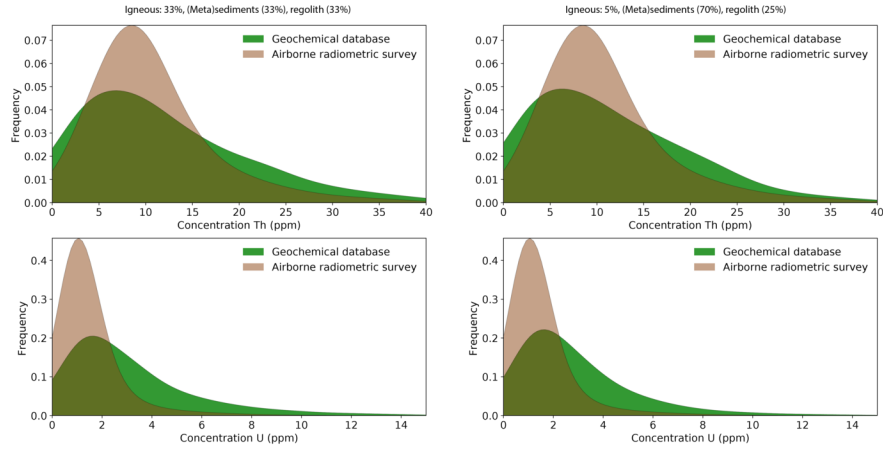
Supplementary Information

Fig. 1 – Simulated distribution for a geochemical data base with different proportions of igneous rocks, (meta)sediments and regolith, in the case of the Northern Pilbara Craton. Note that the effect of varying the proportion of the different lithologies produce marginal modifications of the distributions, and do not resolve the differences in peak position, width and skewness between the airborne distributions and rock samples distributions. This reflects the fact that, distributions of U, and Th, in the various lithologies are, on the first order, similar. Distributions for K are not estimated as the North Pilbara database does not include regolith samples.
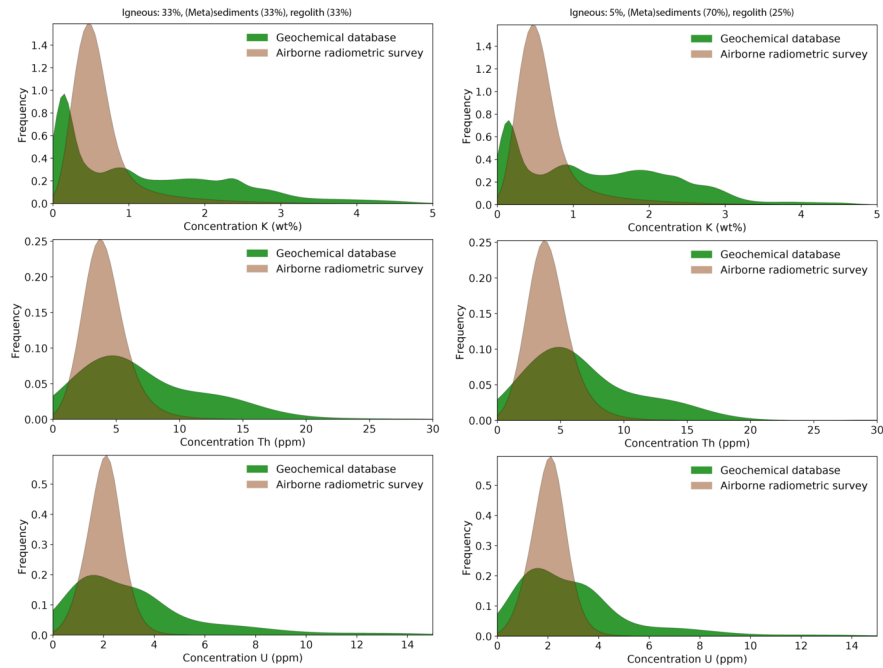

Fig. 2 – Simulated distribution for a geochemical data base with different proportions of igneous rocks, (meta)sediments and regolith, in the case of the West African Craton. As in the Northern Pilbara Craton, Note that the effect of varying the proportion of the different lithologies produce marginal modifications of the distributions, and do not resolve the differences in peak position, width and skewness between the airborne distributions and rock samples distributions. As for the Northern Pilbara Craton, the distributions in the various lithologies are, on the first order, similar, except for K in the regolith. Note that a dominant

2

proportion of regolith (not shown here) does not resolve the differences either, considering the fact that the low K in regolith would not match with the distribution of K in the airborne dataset.

The impact of measurement scale on the univariate statistics of K, Th, and U in the Earth crust

D. Author[1,2], M. Fall[3,4], P.-Y. Meslin[5], M.W. Jessell[6], O. Vanderheaghe[1], J.M. Moyen[7], P.M. Ndiaye[3], K. Boamah[8], L. Baratoux[1,2], and A.-S. André-Mayer[9].

[1] Géosciences Environnement Toulouse, University of Toulouse, CNRS & IRD, 14 Avenue Edouard Belin 31 400 Toulouse.

[2] Université Félix-Houphouët-Boigny, Abdijan, Côte d'Ivoire.

[3] University Cheikh Anta Diop, Geology Department, Dakar, Senegal.

[4] Institut Fondamental d'Afrique Noire Cheikh Anta Diop, Senegal, Dakar.

[5] Institut de Recherche en Astrophysique et Planétologie, University of Toulouse, CNRS & IRD, 9, Avenue du Colonel Roche, 31 400 Toulouse.

[6] Center for Exploration Targeting, School of Earth Sciences, The University of Western Australia.[3]Affiliation for author 3.

[7] LGL-TPE, UJM-UCLB-ENSL-CNRS, 23 rue Dr. Paul Michelon, 42023 Saint Etienne.

[8] Geological Survey Department of Ghana.

[9] GeoRessources, CNRS, Université de Lorraine, France

Corresponding author: David Baratoux (david.baratoux@ird.fr)

Key Points:

- Frequency distributions of K, Th, and U concentrations from airborne radiometric surveys and geochemical databases are compared

- Frequency distributions of K, Th and U concentrations are scale-dependent

- Concentrations of K, Th and Y are heterogeneous at the sub-pixel scale of gridded airborne radiometric maps.

Abstract

The univariate statistics of Potassium (K), Thorium (Th) and Uranium (U) concentrations, in the Earth's oceanic and continental crust are examined by different techniques. The frequency distributions of the concentrations of these elements in the oceanic crust are derived from a global catalog of mid-ocean ridge basalts (MORB). Their frequency distributions of concentrations in the continental crust are illustrated by the North Pilbara Craton, and the West Africa Craton. For these two cratons, the distributions of K, Th and U derived from geochemical analyses of several thousand whole rock samples differ significantly from those derived from airborne radiometric surveys. The distributions from airborne surveys tends to be more symmetric with smaller standard deviations than the right-skewed distributions inferred from whole rock geochemical analyses. Hypothetic causes of these differences include (i) bias in rock sampling or in airborne surveys, (ii) the differences in the chemistry of superficial material, and (iii) the differences in scales of measurements. The scale factor, viewed as consequence of the central limit theorem applied to K, Th and U concentrations, appears to account for most of the observed differences in the distributions of K, Th and U. It suggests that the three scales of auto-correlation of K, Th and U concentrations are of the same order of magnitude as the resolution of the airborne radiometric surveys (50 – 200 m) and concentrations of K, Th, U are therefore generally heterogenous at smaller scales.

Plain Language Summary

Potassium (K), thorium (Th) and uranium, termed together heat-producing elements (HPE) are commonly analyzed in Earth sciences, owing to their faculty to trace various geological processes. The concentrations of these elements may be analyzed in rock samples, or mapped by airborne radiometric surveys (mapping of gamma ray emitted by ^{40}K, ^{232}Th and ^{238}U), which are very different techniques. Here, we reveal that frequency distributions of HPE concentrations estimated from data sets build from these different techniques are different. The possible causes of these differences, including possible biases, atmospheric radon, and scale are investigated. We conclude the scale factor and the heterogeneity of HPE at scales that are typically lower than the footprint of airborne radiometric surveys is the main factor controlling the change in shapes of the frequency distributions. The evolution of asymmetric (right-skewed) frequency distributions toward normal distributions as a function of the volume of an individual analysis is a natural consequence of the Central Limit Theorem.

1 Introduction

Potassium (K), Thorium (Th) and Uranium (U) belong respectively to the groups of Large-Ion Lithophile Elements and High-Field Strength Elements and have difficulties entering in the structure of rock-forming minerals of silicate rocks composing planetary crusts (Cuney 2010 and references therein). Their concentration is known to vary over several orders of magnitudes in the Earth's crust and the three elements can be used as tracers of igneous, hydrothermal and weathering processes. All three are incompatible elements that concentrate in the liquid phase during partial melting or in the residual liquids during fractional crystallization of silicate melts. The mobility of U depends on redox conditions, which has important implications for the secular variations U deposit types as a function of time, considering the strong increase of atmospheric oxygen from 2.4 to 2.2. Ga (Cuney, 2010). It is insoluble in +4 state but soluble in +6 state and thus U is mobile during hydrothermal alteration in contrast to Th that is immobile under the same conditions (Bourdon et al., 2003).

The Th/U is thus a tracer of hydrothermal processes (Kirkland et al., 2015; Rubatto, 2002; Williams et al., 2004). K is generally easily removed from minerals by aqueous alteration. Th is only mobile under acidic conditions (Bullock & Moore, 2004; Langmuir et al., 1980). Therefore, variations of the K/Th ratio may be used as a proxy of the action of surface weathering processes.

Unlike other chemical elements, mapping the concentration of K, Th, U in surface materials can take advantage of the emission of gamma rays associated with the disintegration of their naturally occurring radioisotopes (or with the disintegration of some of their decay products, in the case of Th and U). This disintegration is associated with heat production in the interior of the Earth (crust and mantle), and for this reason, these elements will be termed together, here, and hence after Heat-Producing Elements (HPE). Th is a radioelement with one main naturally occurring isotope ^{232}Th. Potassium has three naturally occurring isotopes, two being stable (^{39}K, ^{41}K), and one being unstable (^{40}K). Uranium as three naturally occurring radioisotopes (^{234}U, ^{235}U, ^{238}U), ^{238}U being the most abundant (99.3 wt% of total U). The decay of ^{40}K and of some of the daughter-elements of ^{232}Th and ^{238}U produces gamma rays that can be measured to infer HPE concentrations in crustal rocks exposed at the surface of the Earth, assuming secular equilibrium between ^{232}Th and ^{238}U and their decay products. Airborne radiometric (gamma ray) surveys have been therefore widely used for regional or high-resolution geological mapping (Dickson and Scott, 1997), since the relative concentrations of K, Th and U in surface material vary over several orders of magnitudes and may be used to delineate lithological boundaries (Dentith & Mudge, 2014; Metelka et al., 2011). The products of radiometric surveys are also amenable to quantitative analyses of HPE concentrations. Example of such studies include the quantitative estimation of heat production in crustal domains, which are then compared with other constraints, such as heat flow measurements (Bodorkos et al., 2004; Phaneuf & Mareschal, 2014; Youssef, 2016). Together with other data sets, airborne radiometric maps are valuable for petrogenetic studies (Tartèse et al., 2011; Xhixha et al., 2016) or for the study of surface processes, as shown by the global map of weathering of Australia produced by Wilford (2012). Gamma rays surveys are also useful for understanding the behavior of Th, and U in granitic complexes (Mohamud et al., 2015).

Given their widespread use, it is worth recalling that the HPE concentrations from airborne data do not necessarily represent the compositions of rocks that would be sampled within the "footprint" of a pixel on an airborne dataset. Indeed, airborne measurements result from the integration of a volume of material, which represents the relative proportions of exposed fresh rocks, soil, or regolith. The different concentrations of HPE in rocks, soils and regolith result from redistributions of these elements owing to magmatic-hydrothermal differentiation and alteration as well as surface processes. Second, the scale of analyses in airborne datasets is several orders of magnitude larger than the typical size of samples analyzed at the laboratory. Laboratory samples are generally prepared as a homogenized powder of the order of hundreds of cm^3 of fresh rocks. The footprint of an airborne acquisition depends on the altitude of the aircraft and is typically ~50-250 m (corresponding to 95% of the collected signal, if measured from a height of 50 m above ground) and a depth of ~30 cm (corresponding to 95% of the collected signal, for a soil density of 1.2 g cm^{-3}) (Dentith & Mudge, 2014; Grasty, 1987), which correspond to a volume of the order of thousands of m^3. In addition, the data are then gridded at a resolution intermediate between the distance between two acquisition points on a flight line and distances between flight lines. The volume of probed material by airborne radiometrics is therefore 6 to 8 orders of magnitude larger than rock samples. The heterogeneity of HPE concentrations at the scale of tens of meter to hundreds of meters is poorly documented, since this would request analyses of numerous samples taken at a few meters from each other. Recently, Fall et al. (2018) and Moyen et al. (2021) explored the spatial pattern of HPE concentrations in rocks, soils and regolith, for different Paleoproterozoic and Archean granites of Senegal and South Africa, respectively. This work suggests that large variations of concentrations may be common at the sub-pixel scale of airborne data, as a result of both magmatic and secondary hydrothermal and/or weathering processes. This work also concludes that the distribution of HPE concentrations over areas of only a few thousands of km^2 may be often right-skewed, at least in the context of these granitoids and their respective climatic contexts of weathering.

The objective of this study is to further investigate the role of the observation scale (the size of an individual sample) on the frequency distributions (or histograms) of HPE concentrations measured by different techniques. Frequency distributions of concentrations of chemical elements on whole rock samples have been investigated 60 years ago with motivations in economic geology (Ahrens, 1954; De Wijs, 1953). Since these seminal studies, it became clear that various types of distributions may be encountered in nature and may be sometimes approximated by normal, log-normal or fractal laws depending on the geological history, which can be described as a superposition of differentiation and mixing processes (Allegre & Lewin, 1995). However, the significance of these investigations was questioned due to the relatively small number of available analyses (typically a few hundreds of geochemical analyses), and due to the heterogeneous spatial distribution of the samples.

In contrast, radiometric surveys provide a large number of regularly distributed HPE concentrations (several millions of "samples"). Such data sets are much more appropriate for a reliable estimation of frequency distributions of HPE concentrations in the crust. This allows us to investigate whether such distributions are comparable with frequency distributions of HPE concentrations that would be obtained from rock samples, despite the differences in scales and considering the nature of sampled material (fresh rock samples versus soil or regolith). To address this question, we have estimated and compared the frequency distributions of HPE concentrations over two regions of the continental crust, the North Pilbara and the West Africa cratons, for which the first order geology is known and both extensive radiometric data and geochemical databases are available. The North Pilbara craton (Australia) is dominated by Archean greenstone belts affected by pervasive metamorphism and hydrothermal alteration delineating large domes cored by granitoids (Kranendonk et al., 2002). The West Africa craton comprises an Archean cratonic nuclei, also made of greenstone belts and granitoids, which is surrounded by Paleoproterozoic volcanic-sedimentary series intruded by granitoid plutons (Milési et al., 1992). Both cratons are affected by intense weathering and regolith development (Chardon et al., 2018; Metelka et al., 2011, 2018; Wilford et al., 2016).

In addition to these statistical studies on the continental crust, we have also examined the frequency distributions of HPE concentrations of the oceanic crust based on a compilation of mid-oceanic ridge basalt compositions (Gale et al., 2013). The distribution of HPE concentrations in the oceanic crust is examined to provide a reference case that is dominated by basalts from partial melting of the mantle and crystallization processes. Though the oceanic crust is also composed of serpentinized peridotite and pervasively affected by hydrothermal alteration, it exhibits a simpler history with respect to the continental crust, which may have been subjected to several episodes of melting, fractional crystallization, hydrothermal alteration and surface processes. This analysis is provided to shed light on the possibly universal characters of the distribution of HPE concentrations in crustal material, which is important to consider when interpreting airborne radiometric surveys elsewhere on Earth.

2 Data sets

2.1 Geochemical data bases

OZCHEM is Geoscience Australia's national whole-rock geochemical database (Champion, 2015). This release of OZCHEM contains over 50000 analyses of rocks, regolith and stream sediments from many regions of Australia. The data are publicly available and were released under the Creative Common License. The locations of the samples selected for this study are reported on a simplified geological map of the Northern Pilbara Craton (Australia) (Figure 1).
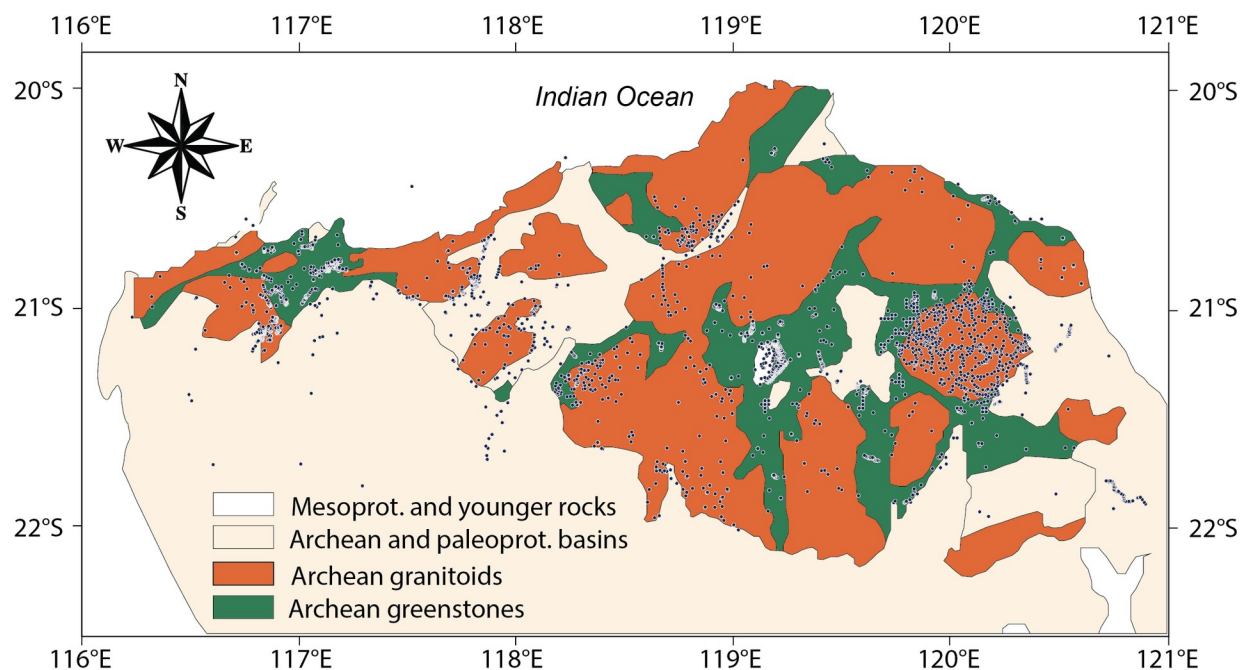
Figure 1 – Sample localities for the OZCHEM geochemical database overlaid on a simplified geological map (cylindrical projection) of the Northern part of the Pilbara Craton adapted from Bodorkos et al. (2004).

The HPE concentrations of the West Africa Craton have been extracted from the West African Exploration Initiative database. This database contains of compilation of geochemical data acquired during the course of the West Africa Exploration Initiative project. The results of this research program have been progressively published over the last ten years in four special issues at the end of the confidentiality for stage two of the project (Goldfarb et al., 2017; Hein, 2016; Jessell et al., 2016; Jessell & Liégeois, 2015). The location of these samples are also reported over a simplified map of the West Africa Craton based on the map published by (Baratoux et al., 2011).
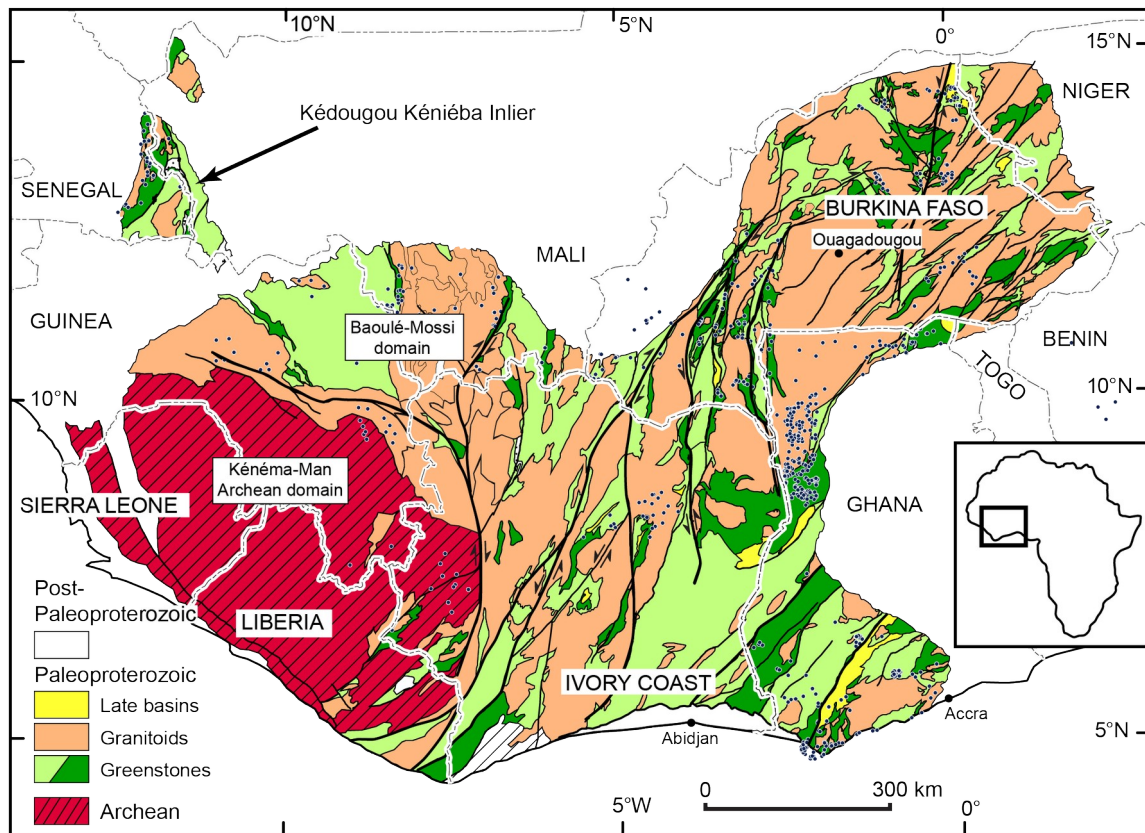

Figure 2 - Sample localities (blue circles) for the WAXI Geochemical database overlaid on a simplified geological map (cylindrical

The HPE concentrations of mid-oceanic ridge basalts were extracted from the compilation by Gale et al. (2013). This compilation contains 33,695 samples, taken from several published and unpublished databases, and were filtered to eliminate questionable or inapplicable analyses and retain only the highest-quality data (see Gale et al., (2013), for the details about the selection of samples and analyses).

2.2 Airborne radiometric surveys

For the Australian crust, the HPE concentrations are extracted over the northern part of the Pilbara Craton from the radiometric map of Australia (Minty et al., 2008). A RGB representation of the area of interest is given in Fig. 3. The norther Pilbara is essentially desert, and airborne radiometrics are not affected by vegetation. For the West African Craton, the HPE concentrations are derived from airborne radiometric surveys provided by the Geological Survey of Ghana (Fig. 4). South of Ghana is covered by vegetation, whereas the vegetation in northern part, with a Sahelian climate is sparse. HPE concentrations are extracted over the paleoproterozoic units of Ghana. In the case of the Northern Pilbara craton, the same areas, delineated in Fig. 3, have been used for the extraction of radiometric data and geochemical data. In the case of the West African Craton, the number of rock samples over the Paleoproterozoic units of Ghana are not large enough for statistical analyses. We have therefore used the entire WAXI geochemical database, which contains samples from paleoproterozoic and archean units of the West African Craton.
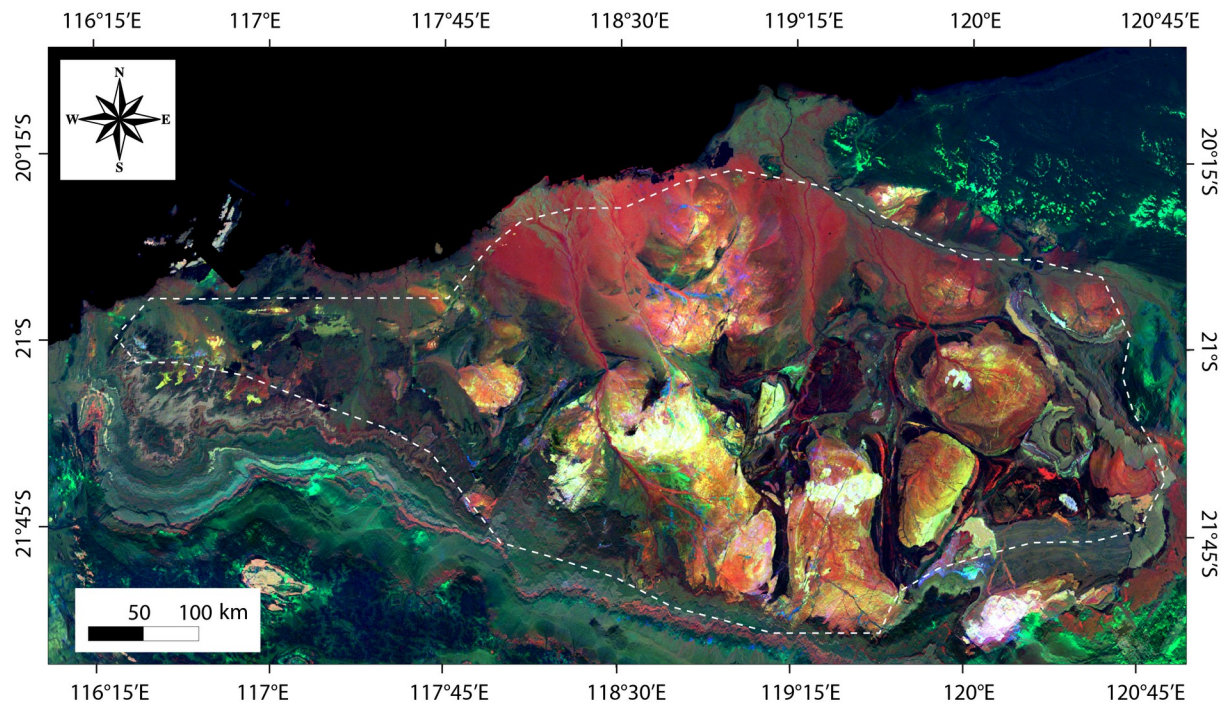

Figure 3 - RGB representation of HPE concentrations over the Northern part of the Pilbara Craton, Western Australia, extracted from the radiometric map of Australia (Minty et al., 2008). Red = Potassium (0 to 5wt%), Green = Thorium (0 to 40 ppm), Blue = Uranium (0 to 7 ppm). Concentrations within the dotted white line, encompassing most of the archean greenstones and granitoids, are extracted for the estimation of the distributions.
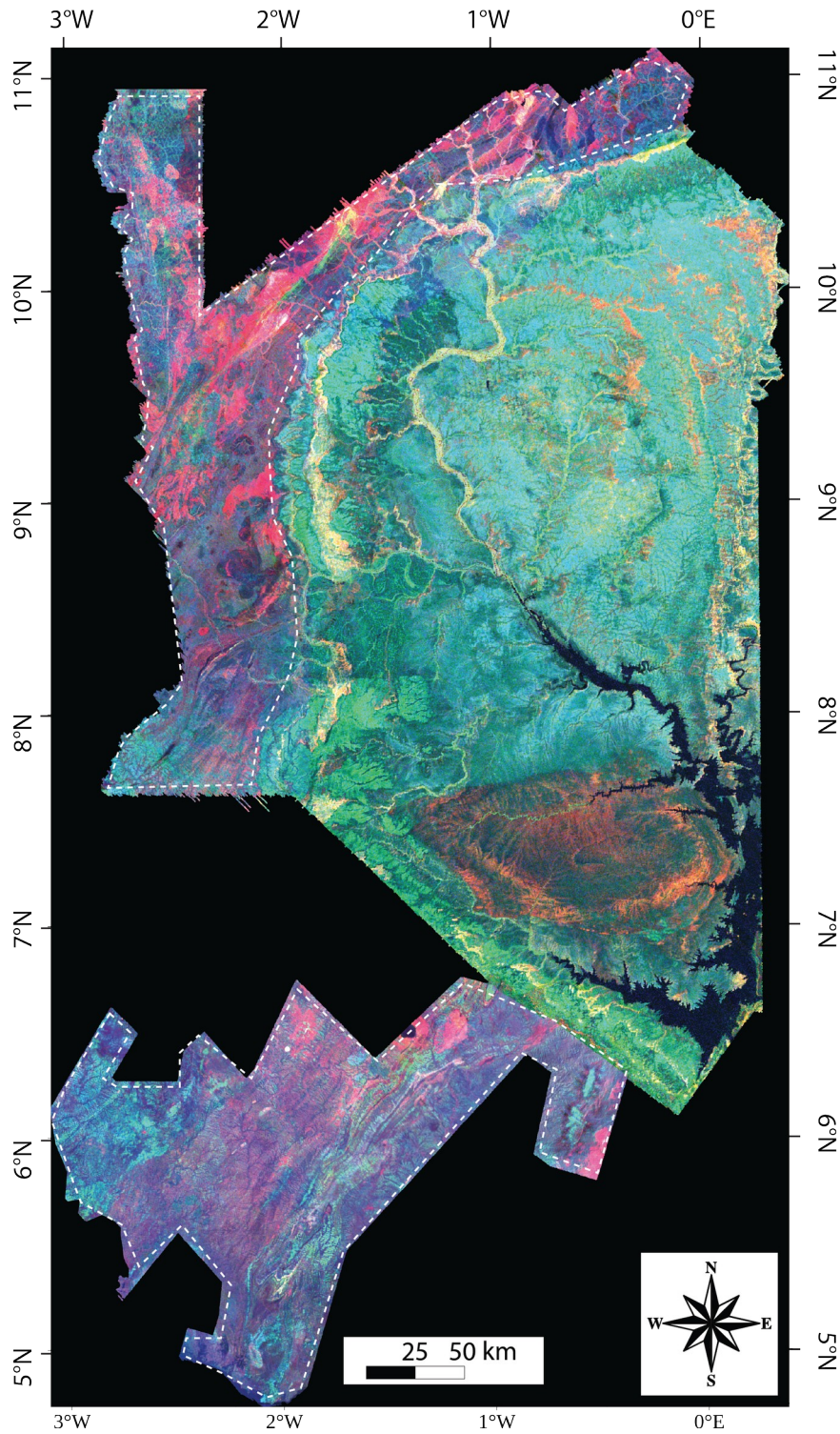
Figure 4 - RGB representation of the HPE concentrations from the radiometric map of Ghana Concentrations within the dotted while line (corresponding to the Paleoproterozoic units in Ghana) are extracted for the estimation of the distributions. Red = Potassium (0 to 2wt%), Green = Thorium (0 to 10 ppm), Blue = Uranium (0 to 4 ppm). Note that the color scales are different

with respect to Fig. 3, since the West African Craton exhibits lower concentrations in K, Th and U than the Pilbara craton.

3 Methods for the estimation of the frequency distributions of HPE concentrations

HPE concentrations are treated here as random variables for which the probability density function must be estimated from a finite number of observations. Histograms are the simplest non-parametric density estimators. They are frequently encountered but have several disadvantages: they are not continuous functions and they depend on the end points and widths of the bins. We chose here to use their generalization, the kernel density estimators (Rosenblatt, 1956), which alleviate these problems. The kernel density estimation is generally considered to be a more robust statistical approach to estimate probability density functions from a finite number of data and is therefore applied here to both HPE concentrations from geochemical databases and from airborne radiometrics.

Consider a set of n concentrations (C_1, C_2, ..., C_n) for which we want to estimate the probability density function f(C). Its kernel density estimator is given by:

$$\overline{f}(C) = \frac{1}{nh} \sum_{i=1}^{n} K(\frac{C - C_i}{h})$$

(1)

where K is the kernel - a non-negative function that integrates to one - and h is the smoothing parameter called the bandwidth, which correspond to the smallest interval of concentrations for which variations in the frequency distribution would have a physical meaning (i.e., do not correspond to statistical noise). The bandwidth must be larger than the measurement error. The results are dependent on the bandwidth and of the kernel, which is generally a Gaussian function. If the bandwidth is too narrow, the resulting density is rough and noisy (variations results from the small number of samples integrated by the kernel). When the bandwidth is too large, real features of the underlying distribution may be smoothed away. Various methods have been developed for automatic selection of the bandwidth based on the dataset itself (Jones et al. 1996). Alternatively, it is possible to achieve a manual selection of the bandwidth based on the visual examination of the resulting distributions. Moreover, the objective of the investigation is to compare distributions estimated from different data sets. It is therefore important to keep the bandwidth constant among the analyses of different data sets, in order to highlight possible differences in the distributions that are directly related to the dataset, and do not from differences in numerical treatment. We have therefore chosen minimal values for the bandwidth that are commensurate with the accuracy of the concentrations for the different techniques, *i.e.* 0.1 wt% for K, and 1 ppm for U and Th, and avoid the risk of smoothing away physical fluctuations of frequencies.

In order to highlight the possible normal or log-normal characters of the distributions, we also apply the kernel density estimation to the logarithm of the concentrations. The choice of the bandwidth was empirically determined. As for the linear scale of concentration, it is important to use the same bandwidth for both the radiometric data sets and for the geochemical databases. The selected values are log(1.25) for K, log(1.1) for Th and U, with the exception of mid-oceanic ridge basalt for which we retain a value of 1.1 for all HPE.

4 Results

4.1 Distribution of HPE in the oceanic crust

The distribution in the oceanic crust database displays a peak at 0.10 - 0.12 wt% for K whereas Th or U concentrations lower than 0.5 ppm largely dominate the distribution. The distributions of the three elements are right-skewed and are best approximated by log-normal laws, as shown by the least-square adjustment and the more symmetric shapes of the distributions in the logarithmic scales of concentrations.
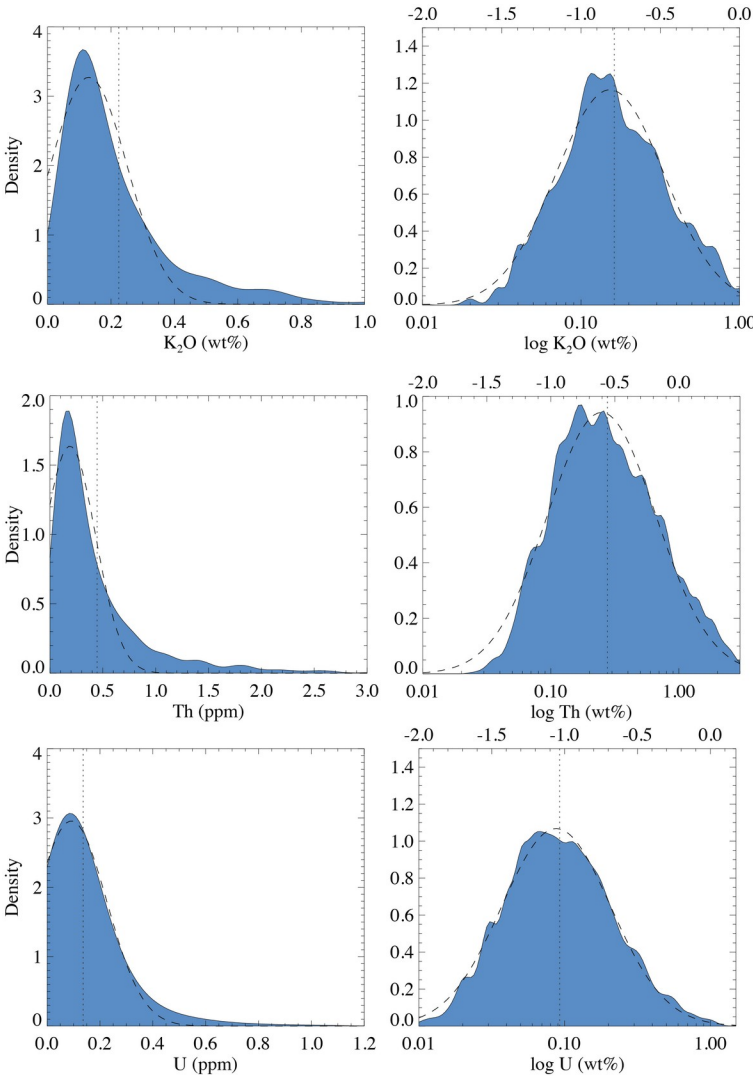

Figure 5 – Frequency distributions of K (upper), Th (middle), and U (lower) concentrations for the oceanic crust in linear (left) and logarithmic scales of concentrations (right), based on the database of geochemical analyses of mid-oceanic ridge basalts (Gale et al. 2013). The dotted curves correspond to a Gaussian function adjusted by the least-squared method. Vertical short-dotted lines indicate the mean values of the distributions (see also Table 1).

Mid-oceanic ridge basalts		
	Geochemical Database	
	Linear scale	Log scale

K$_2$O	*h*	*0.1 wt%*	*1.4*
	Mean (wt%)	0.22 wt%	0.16 wt%
	Standard deviation	0.23 wt%	2.19
	Skewness	3.84	0.24
Th	*h*	*0.1 ppm*	*1.1*
	Mean	0.44 ppm	0. 28 ppm
	Standard deviation	0.58 ppm	2.56
	Skewness	4.93	0.34
U	*h*	*0.1 ppm*	*1.1*
	Mean	0.14 ppm	0.09 ppm
	Standard deviation	0.16 ppm	2.33
	Skewness	5.96	0.27

Table 1 – Characteristics of the distributions of HPE concentrations in the oceanic crust. For each element, the parameter h used for the kernel density estimation is given on the first line (*italicized*), h is given as the multiplicative factor for the logarithmic scale. For the log scale, the mean value corresponds to the geometric mean of the concentrations (in concentration units), and the standard deviation is the geometric standard deviation factor (multiplicative factor) and is dimensionless.

4.2 Distributions of potassium, thorium and uranium in the North Pilbara and West Africa cratons

K and Th distributions of the North Pilbara and West Africa cratons from the two geochemical databases are right-skewed (Figs. 6,7). The much wider range of HPE concentrations than in the oceanic crust reflects the much wider diversity of lithologies and superposition of geological processes (magmatic, hydrothermal and surface processes). However, these distributions are also dominated by K-poor, Th-poor and U-poor rocks. The high Th/U in the Northern Pilbara craton is a characteristics of old, mature, weathered continental crust with massive loss of U (Carpentier et al. 2013). The distributions from the geochemical databases are also right-skewed, but the adjustment to a log-normal distribution is less successful. The more complex behavior may be also induced in part by the superposition of geological processes. The smaller number of samples, in comparison with the oceanic crust database, may also account from some of the irregularities of the distributions. The three elements display similar behaviors in the two cratons, with a broad peak at low concentrations value, and a long tail of elevated concentrations. The distributions from the airborne radiometric surveys do not coincide with those of the whole rock samples in geochemical databases. The average values of concentrations from whole rock samples and airborne data are often similar with two exceptions, U for the North Pilbara Craton, K for the West Africa Craton. In these two cratonic domains, lower average values are reported for the airborne data. The most prominent differences between distributions from airborne surveys and rock samples are a higher concentration for the peak value (mode), a lower standard deviation and a shorter tail in the airborne data. The airborne-based distributions tend to also be right-skewed, but show lower skewness in linear scales of concentrations and produce a better adjustment to the log-normal distribution in the case of K and Th. It is not possible to determine which law provides the best adjustment to U concentrations from the airborne radiometrics. The initial complexity of the distributions from rock samples (multiple peaks, plateau, clear deviations from both normal or log-normal laws) has been lost in the distributions from the radiometric surveys.
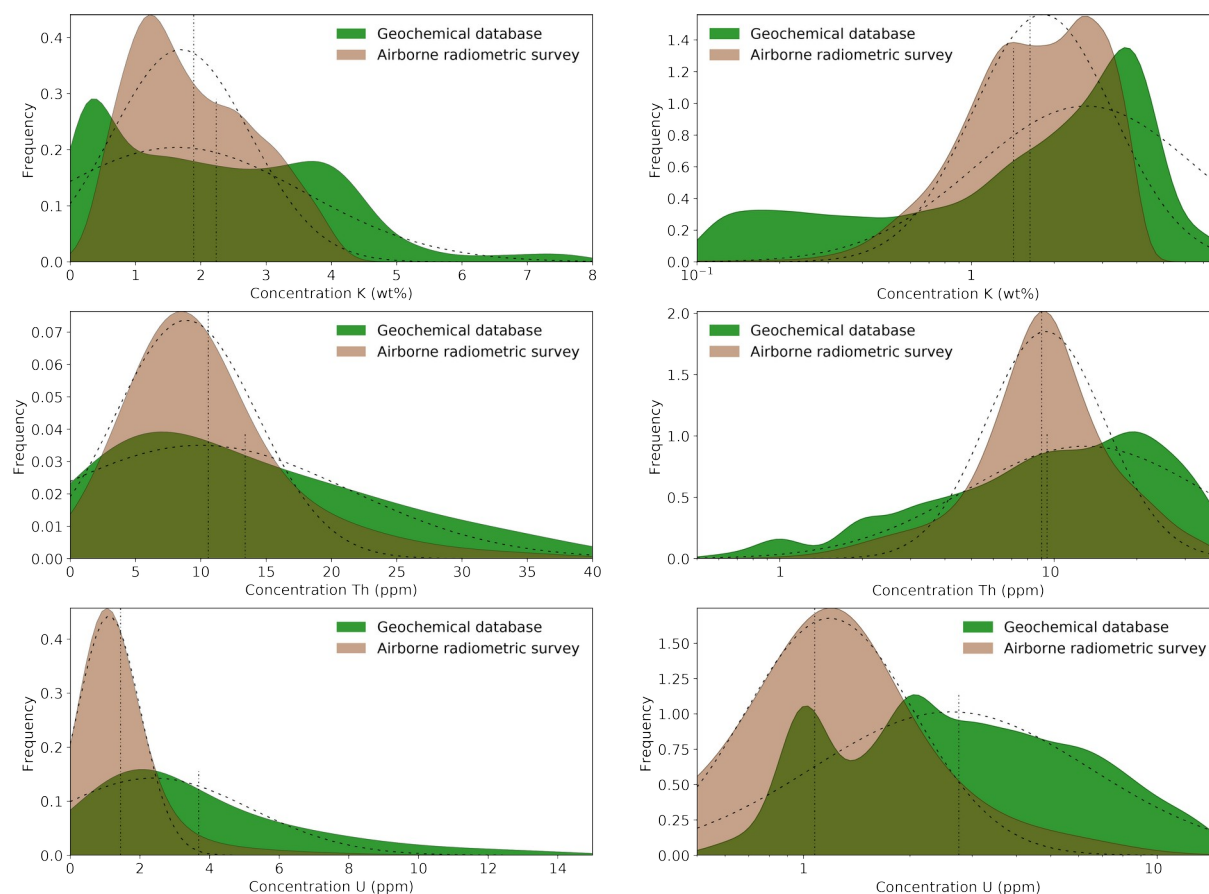
Figure 6 – Frequency distributions of HPE concentrations for the North Pilbara Craton, in linear (left) and logarithmic scales of concentrations (right). Green distributions are obtained from the OZCHEM database (10018, 7558 and 7714 samples have been used for the distributions of K, Th and U, respectively). Grey distributions are obtained from airborne radiometrics. The dotted curves correspond to a Gaussian function adjusted by the least-squared method. Vertical short-dotted lines indicate the geometric mean values of the distributions (see also Table 2).

		North Pilbara Craton			
		Geochemical Database		Airborne radiometrics	
		Linear scale	Log scale	Linear scale	Log scale
K_2O	*h*	*0.1 ppm*	*1.1*	0.1 wt%	1.1
	Mean	2.14 wt%	1.27 wt%	1.95 wt%	1.70 wt%
	Standard deviation	1.73 wt%	3.71	0.92	1.72
	Skewness	1.25	-1.50	0.38	-0.76
Th	*h*	*1 ppm*	*1.25*	1 ppm	1.25
	Mean	10.58 ppm	6.93 ppm	11.36 ppm	9.75 ppm
	Standard deviation	9.27 ppm	2.85	7.15 ppm	1.72 ppm
	Skewness	1.78	-0.96	2.48	0.04
	h	*1 ppm*	*1.25*	*1 ppm*	*1.25*

U	Mean	2.53 ppm	1.79 ppm	1.47 ppm	1.13 ppm
	Standard deviation	2.72 ppm	2.43	1.27 ppm	2.06
	Skewness	2.45	-0.55	3.23	-0.18

Table 2 - Characteristics of the distributions of HPE concentrations in the continental crust based for the North Pilbara Craton. For each element, the parameter h used for the kernel density estimation is given on the first line (*italicized*), h is given as the multiplicative factor for the logarithmic scale. For the log scale, the mean value corresponds to the geometric mean of the concentrations (in concentration units), and the standard deviation is the geometric standard deviation factor (multiplicative factor) and is dimensionless.
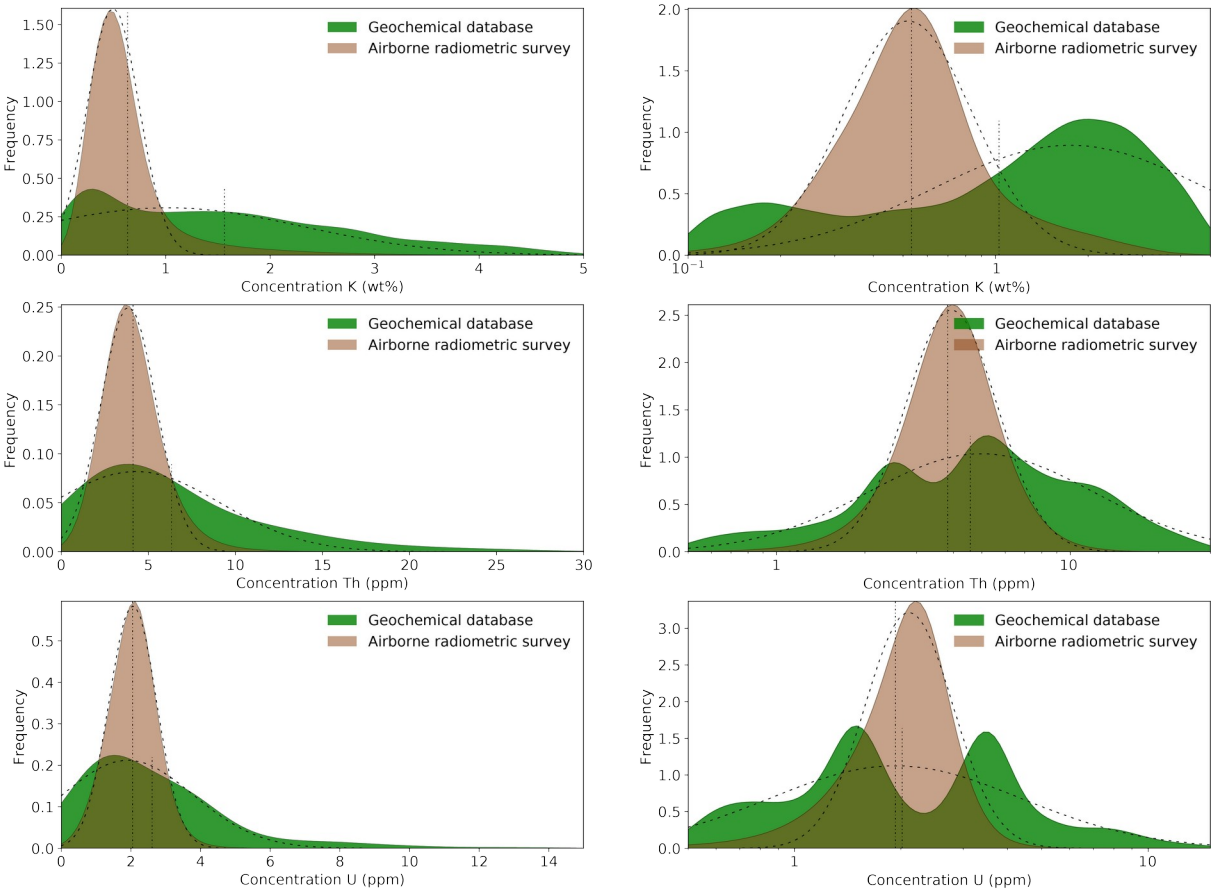

Figure 7 – Frequency distributions of K, Th, and U concentrations for the West Africa Craton. Brown distributions are obtained from the WAXI database (2474, 1814 and 1471 samples have been used for the distributions of HPE, respectively). Grey distributions are obtained from airborne radiometrics. The dotted curves correspond to a Gaussian function adjusted by the least-squared method. Vertical short-dotted lines indicate the mean values of the distributions (see also Table 3).

West Africa Craton				
	Geochemical Database		Airborne radiometrics	
	Linear scale	Log scale	Linear scale	Log scale

		0.1 wt%	1.1	0.1 wt%	1.1
K$_2$O	*h*	*0.1 wt%*	*1.1*	*0.1 wt%*	*1.1*
	Mean	1.68 wt%	0.83 wt%	0.63 wt%	0.53 wt%
	Standard deviation	1.54 wt%	4.47	0.45 wt%	1.77
	Skewness	1.53	-0.41	2.91	0.20
Th	*h*	*1 ppm*	*1.25*	*1 ppm*	*1.25*
	Mean	5.72 ppm	3.22 ppm	4.13 ppm	3.83 ppm
	Standard deviation	6.09 ppm	3.49	1.63 ppm	1.49
	Skewness	3.07	-0.94	1.39	-0.53
U	*h*	*1 ppm*	*1.25*	*1 ppm*	*1.1*
	Mean	2.15 ppm	1.21 ppm	2.05	1.93 ppm
	Standard deviation	2.24 ppm	3.52	0.64	1.45
	Skewness	2.47	-0.90	0.26	-1.55

Table 3 - Characteristics of the distributions of HPE concentrations in the continental crust based for the West Africa Craton. For each element, the parameter h used for the kernel density estimation is given on the first line (*italicized*), h is given as the multiplicative factor for the logarithmic scale. For the log scale, the mean value corresponds to the geometric mean of the concentrations (in concentration units), and the standard deviation is the geometric standard deviation factor (multiplicative factor) and is dimensionless.

5 Origins of the differences between the distributions from airborne radiometrics and geochemical databases

First, it is of note that frequency distributions of HPE concentrations are right-skewed in the three crustal domains investigated here. In the oceanic crust, the frequency distributions are well approximated by a log-normal behavior. The distributions in the cratonic contexts appear to be more complex but also exhibit a large degree of asymmetric (or large skewness). The more complex behavior may result in part from the superposition of multiple geological processes, and from the relatively smaller number of samples in the cratonic domain with respect to the oceanic domain. Second, similar behaviors are observed for the two cratonic domains, when comparing distributions of HPE from rock samples with those from the airborne surveys. This suggests that a common explanation can be found for these differences. Three possible causes will be examined. This first plausible explanation is the fact that rock samples or airborne radiometrics are possibly biased toward higher or lower concentrations in either K, Th or U. The fact that airborne surveys are affected by environmental factors (humidity, radon) and measure shallow material, which corresponds often to soil and/or regolith (sometimes covered by vegetation), and not to fresh rock samples, will be considered here. Bias in geochemical databases may be the consequence of the over or under-representations of the various types of lithologies in the geochemical databases, with respect to the airborne surveys, which produce a regular grid of concentrations of material at the surface. A second possible source of differences is related to the environmental factors in airborne radiometric (vegetation cover, soil humidity, atmospheric radon), which affects the apparent concentrations of HPE. The third possible source of differences between distributions is the scale of measurements, which, as recalled in the introduction of this study, differs by several orders of magnitude.

5.1 Possible biases in the airborne surveys

Airborne survey provides maps of HPE concentrations in the superficial material (up to a few tens of centimeters depth). Depending on the context (climate, erosion rate, rock ages), the airborne radiometric signal come from superficial material that may be either composed of fresh rocks (outcrops), soil (superficial layer composed or organic matter, clays and organisms that support life), regolith, or a mixture of all three categories within a pixel of the map. Soil and regolith, except when transported from a distant site, generally reflects the composition of the underlying rocks with chemical modifications, such as addition of organic material (for soil), removal of mobile elements and accumulation of immobile elements (by mass balance) in the regolith. Soil may also include more humidity than fresh rocks. The addition of organic matter, the presence of a vegetation cover and humidity tends to reduce the observed concentration of HPE with respect to the underlying bedrock. Variations of soil humidity or concentration of organic matter would tend to broaden the frequency distributions of HPE concentrations. Therefore, the presence of soil cannot explain the higher modes of K and Th (Northern Pilbara, Fig. 6), K and U (WAC, Fig. 7) and narrower peaks for all elements in the airborne data. It is therefore possible to exclude the possibility that differences in distributions are the sole consequence of the soil cover that dominates the airborne datasets.
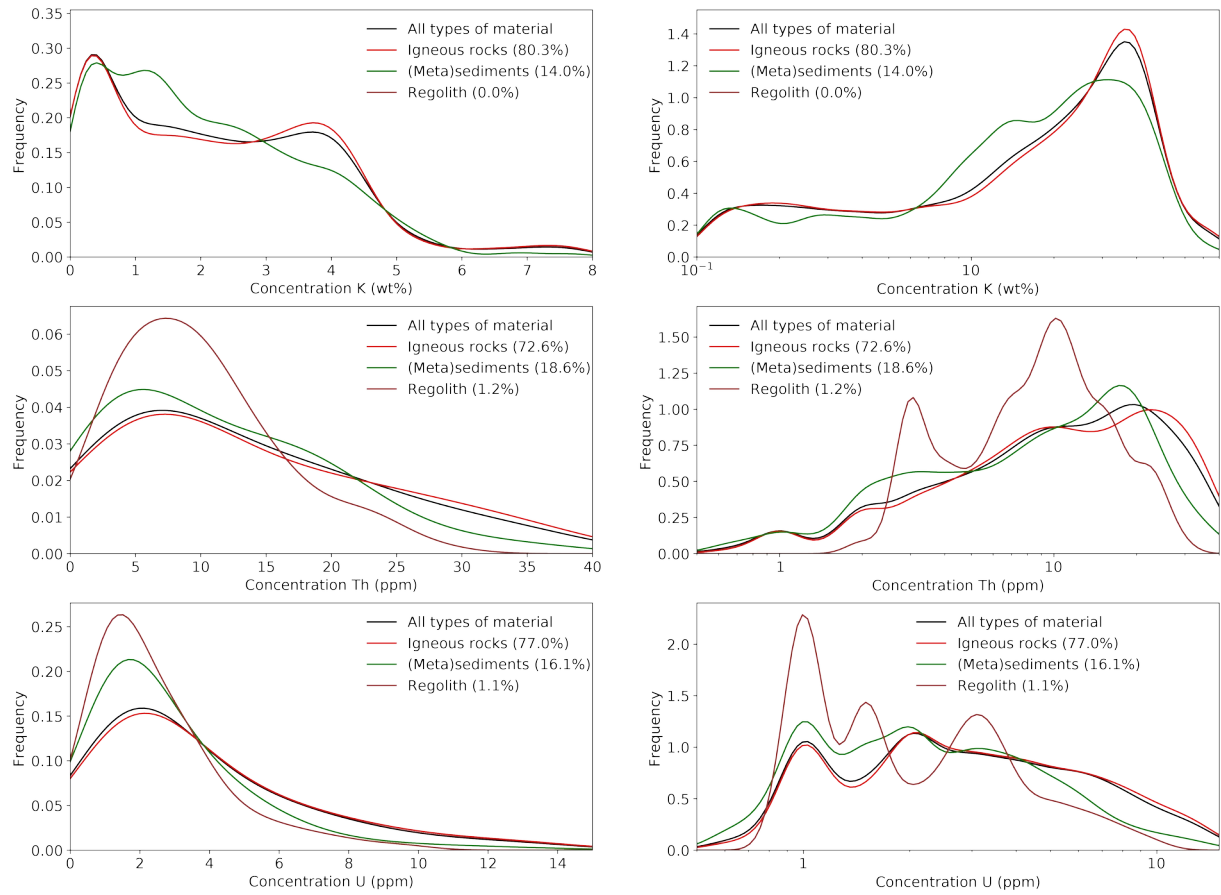
These data are generally provided as gridded data set, for convenience, and the interpolation step induces additional smoothing to the original data. The effects of the interpolation step on frequency distribution of HPE has been investigated previously by comparing frequency distributions from individual measurements (along flight lines) and from concentrations extracted from gridded data at the same location. It was concluded that the frequency distributions are visually indistinguishable (M.W. Jessell et al. 2018, p836).

Last, the presence in the atmosphere of Radon (^{222}Rn) affects the apparent concentrations of U, depending if/how Rn corrections are made for each survey. ^{222}Rn is a gas that is produced in rocks (it belongs to the decay chains of ^{238}U) and its concentration in the atmosphere may vary as a function of surface sources, winds, and precipitation. The presence of ^{222}Rn is therefore responsible for over-estimation of U concentrations in the ground. Variable concentration of atmospheric ^{222}Rn would induce a broadening of the distribution of U concentrations in airborne datasets. For the both the Northern Pilbara and WAC, the distribution of U exhibits a narrower peak and a lower average concentration in airborne data when compared to the U distribution in the geochemical database. We therefore conclude that the presence of ^{222}Rn in the atmosphere is not responsible for the differences in the distribution of U concentrations, whereas it is not excepted to affect the measured concentrations in Th and K.

5.2 Possible biases in the geochemical databases

Airborne surveys produce a regular grid of analyses, and all lithologies are represented as a function of their surface area of exposure at the surface. In contrast, rock samples are heterogeneously distributed and certain types of lithologies may be over or under-represented in the geochemical databases. Regolith, which is generally depleted in K but and enriched in Th will be under-represented in geochemical databases, with respect to the actual spatial fraction of the surface with regolith cover.

In order to determine the consequences of possible sampling biases, the distributions of HPE concentrations from the geochemical databases have been represented for 3 main types of rocks: regolith, sedimentary rocks and their metamorphic equivalents (labelled together as (meta)sediments), and igneous rocks (plutonic and volcanic rocks) (Fig. 8 and Fig. 9). The frequency distributions are normalized, and the proportions of each type of rocks in the all-rocks frequency distributions are indicated for each element. The geochemical databases are clearly dominated by igneous rocks. The (meta)sediments are the second family of rocks represented in the databases, and, regolith is under-represented. In order to determine if this bias could account for the differences between the frequency distributions, the following question must be addressed: is there a category of rocks for which the distributions of the three elements together provide a better match to the distributions from the airborne data? For the northern Pilbara, comparison of Fig. 6 and Fig. 8 indicate that (meta)sediments offer a better match to the airborne distribution for K and U, but not for Th. The distribution of Th in regolith is close to that of Th in the airborne distribution. However, despite the fact that K concentrations in regolith are not available for this database, the general depletion of K in regolith is not able to account for the higher mode of the frequency distribution of K in airborne data. Therefore, neither an under-representation of (meta)sediments or regolith without respect to the igneous rocks would explain the differences in the distributions for the Northern Pilbara. The same exercise may be achieved for the West African Craton, by comparing Fig. 7 and Fig. 9. Here, under-representation of regolith in the database could account for differences in the distribution of K, but not for U, and Th (wide, right-skewed distribution of U and Th in regolith). The broad distributions of K in metasediments cannot account for the narrow and lower mode of the distribution of K in the airborne data. To further confirm these assertions based on qualitative examination of the distributions for each lithologies, we produced frequency distributions of K, Th and U concentrations for modified proportions of igneous rocks, (meta)sediments and regolith (Supplementary Information, Fig. 1 and Fig. 2). None of these attempts are able to reproduce both the distributions observed in K, Th and U.

Fig. 8 - Frequency distributions of K, Th, and U concentrations for the Northern Pilbara as a function of three main rock types: igneous, (meta)sediments and regolith. Note that K concentrations in regolith are not available in the Ozchem database for Western Australia.
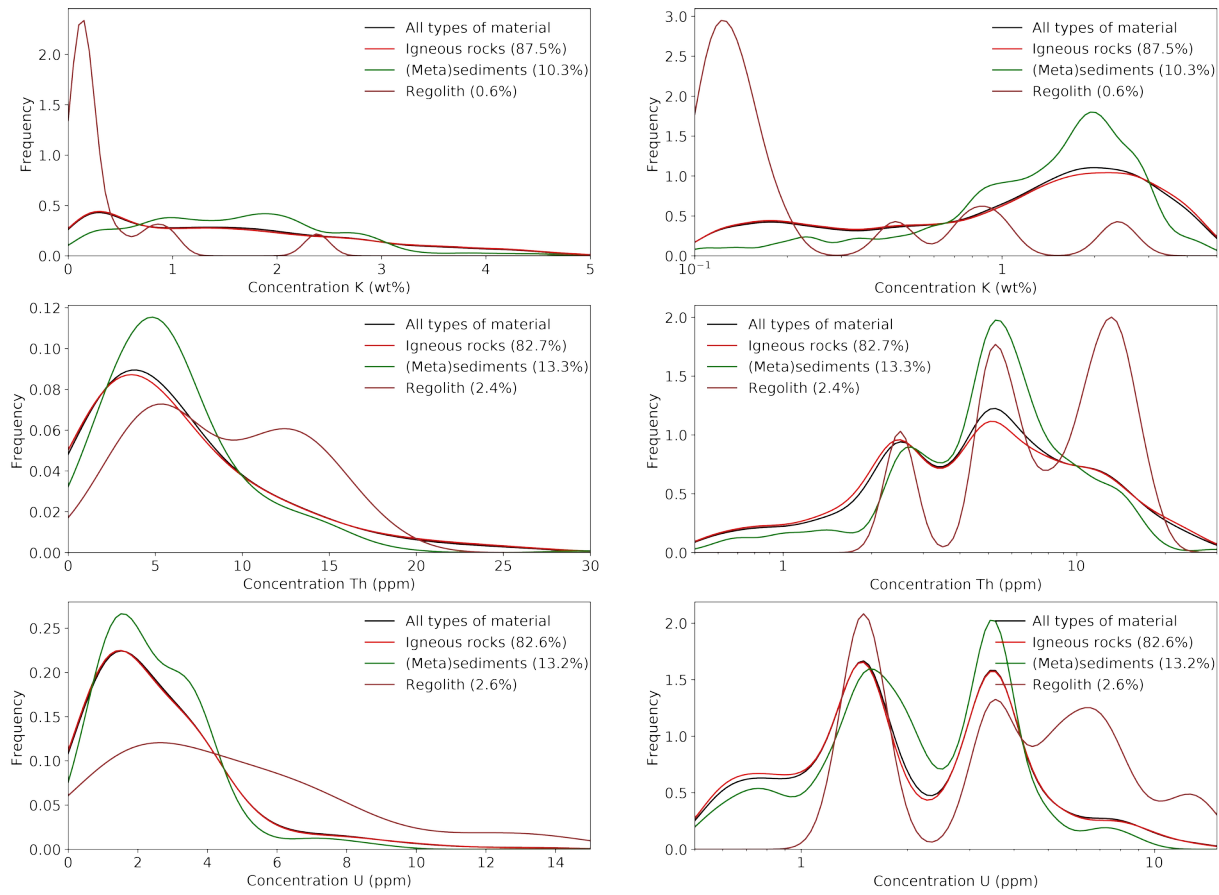
Fig. 9 - Frequency distributions of HPE concentrations for the West Africa Craton as a function of three main rock types: igneous, (meta)sediments and sediments and regolith. Note that peaks in Th and U distributions in the logarithmic scale are artefacts resulting from the small number of regolith samples in the database and of the precision of Th and U concentrations.

5.3 The scale factor

Here we explore if the differences between airborne data sets and geochemical databases are the consequences of the variations of the concentrations at scales smaller than the resolution of the airborne survey. Let us assume that the concentrations of either K, Th or U is a random variable or the result of a stochastic process. Indeed, at each location, the concentration of each element is considered to be the consequence of the superposition of igneous and secondary processes (metamorphism, hydrothermal alteration, weathering, erosion, transport, sedimentation) which can operate everywhere within the random field. Let us also assume that the concentrations of any of the three elements become independent beyond a certain distance. In spatial geostatistics, this distance corresponds to the range of the empirical variogram. The central limit theorem states that the distribution of the sum of a series of independent random variables tends toward the normal distribution, even if the random variables themselves are not normally distributed.

The numerical simulations, described below, illustrate the consequence of the central limit theorem, when applied to distributions of concentrations of K, Th or U from geochemical databases (rock samples) and from airborne radiometric data. For the simulation, it is assumed that concentrations are spatially independent variables with a log-normal behavior at a scale intermediate between the sample scale (the typical size of a rock sample) and the scale of the pixel of an airborne survey. The choice of the log-normal behavior is justified by the excellent approximation of the log-normal law for the K, Th and U concentrations in the oceanic crust, the right-skewed distributions for HPE in the cratonic domain, the theoretical considerations that log-normal distributions are natural consequences of the geochemical behavior of HPE in magmatic processes (Allegre & Lewin, 1995). This frequency distribution of concentrations is labelled F(C) and the sample scale is noted s. In other words, the hypothesis is made that the range of the empirical variogram of HPE is (i) greater than the typical rock sample scale, but (ii) lower than the resolution of the airborne data set. It is of note that the second part (ii) of this assumption may not be rigorously verified, as ranges in empirical variograms of HPE concentrations of the order of a few hundreds of meters to a few kilometers have been reported in felsic domains (Fall et al. 2020; Moyen et al. In press). The scale-dependent effects observed in nature may be therefore less pronounced than the scale-dependent effects illustrated below, achieved under the assumption of a rigorous independence of concentrations at scales lower than the resolution of the airborne data. The log-normal law is characterized by two parameters, the expected value (μ) and standard deviation (σ). The resolution of the survey is called δ and the area of the survey is called A (m^2). The number of pixels in the gridded survey of resolution $\square$ is $n = A/\delta^2$. The concentration in each pixel of the airborne survey is determined from the average value of random draws of concentrations based on the statistical law F(C):

$$F(C) = \frac{1}{C\sigma\sqrt{2\pi}} \exp\left(\frac{[\ln(C) - \ln(\mu)]^2}{2\,s\sigma^2}\right) \qquad (1),$$

where μ represents a concentration and is arbitrarily chosen to 0.3 (the values of the x-axis may be multiplied by any factor, without any consequences on our conclusion. The parameter $\square$ is chosen to produce of right-skewed distribution with a skewness comparable to skewness values observed in natural concentrations. For a value of $\square$ of 0.5, the skewness (5.05) is determined using the following formula:

$$skewness = (e^{¿¿}\sigma^2 + 2)\sqrt{e^{\sigma^2} - 1}\,¿ \qquad (2).$$

The number of random draws is equal to $(\delta/s)^2 = r^2$, where r is the scale ratio. This scale ratio r represents the ratio between the scale at which the concentration of the chemical elements is spatially independent and controlled by the log-normal distribution F(C), and the resolution of the airborne survey. The simulated "rock samples" frequency distribution (geochemical database) is determined from a random draw of the concentrations in n samples, based on the statistical law F(C). The simulated "airborne survey" frequency distributions may be then compared with each other as a function of the scale ratio (Fig. 10) and with the "rock samples" distribution F(C). Fig. 10 illustrates effects on the distributions that are qualitatively comparable to the observed differences between the distribution from geochemical databased and airborne survey on the continental crusts. The geochemical database distribution shows relatively large fluctuations around the log-normal distribution F(C), which is the consequence of the small number of samples (n = 100) used to generate this distribution. The frequency distributions of the airborne surveys tend toward the normal distribution with increasing values of the scale ratio and complexity, and the presence of secondary peaks, is progressively erased.
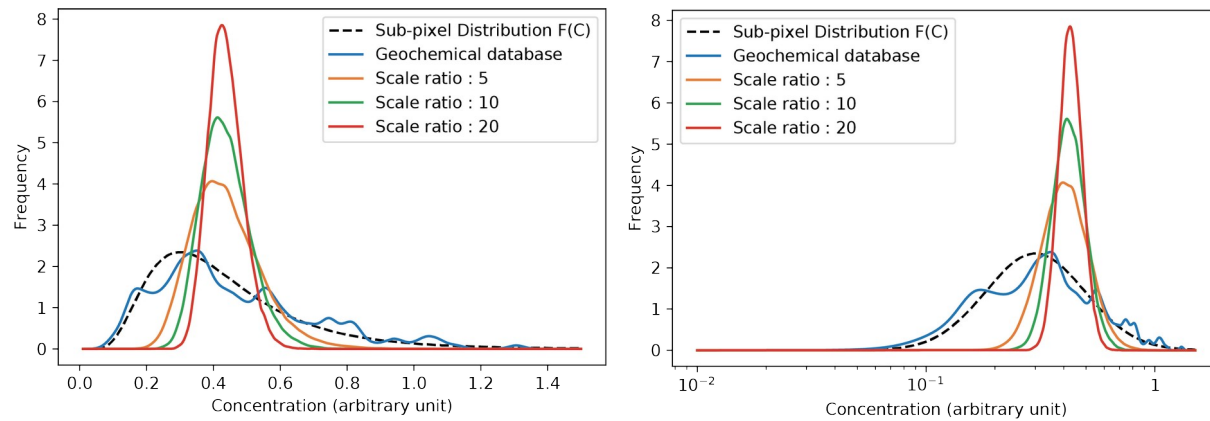

Fig. 10 – Simulation of the effect of the scale of measurement on the observed frequency distributions of concentration. The simulation was achieved using a log-normal distribution for F(C) (μ= 0.3, σ = 0.5); n = 100 (number of samples in the geochemical database) and n' = 50000 (number of pixels in the airborne survey). The distributions are given as a function of concentration in linear scale in the left panel, and in logarithmic scale in the right panel. Given the evidence that HPE concentrations vary at scales smaller than the resolution of airborne survey (Fall et al., 2018, 2020; J-F. Moyen et al., 2021), we therefore conclude that the distribution of the concentrations of HPE in the continental crust are affected by the scale of measurement.

6. Conclusion: Implications for the interpretation of airborne datasets

The frequency distributions of HPE concentrations in the continental crust appears to be scale-dependent. The average values of HPE concentrations are naturally independent of scale but the other moment of these variables (e.g., standard deviation, skewness) are scale-dependent. At small scale (rock samples, a few tens of cm^3), the distributions are right-skewed and may be approximated by the log-normal law. At the scales typical of radiometric surveys (individual samples, or pixels, in the order of tens of thousands of m^3), the distributions tend of be more symmetric (normal law). This scale-dependence is the natural consequence of the Central Limit Theorem applied to HPE concentrations in the Earth crust. The importance of this effect is controlled by the distance of spatial auto-correlation of HPE concentrations, which may vary from one element to the other. Quantitative interpretations of airborne radiometric surveys are combined with different sources of information in many applications (geological mapping, mineral exploration, geothermal projects). Such applications must therefore carefully consider the scale transfer problem when integrating different sources of data for HPE concentrations. The relatively short distances of spatial auto-correlations (or the relatively large degree of heterogeneities of concentrations over short distances) of the three elements is a direct consequence of their geochemical behavior (incompatible elements for HPE, and immobility of Th and U in many contexts). This behavior may be tentatively extrapolated to other minor or trace elements with similar geochemical behavior. The existence of relationships between univariate and spatial statistics and geochemical behavior is a relatively unexplored area of research which will be explored in future studies.

6. Conclusion: Implications for the interpretation of airborne datasets

The frequency distributions of HPE concentrations in the continental crust appears to be scale-dependent. The average values of HPE concentrations are naturally independent of scale but the other moment of these variables (e.g., standard deviation, skewness) are scale-dependent. At small scale (rock samples, a few tens of cm^3), the distributions are right-skewed and may be approximated by the log-normal law. At the scales typical of radiometric surveys (individual samples, or pixels, in the order of tens of thousands of m^3), the distributions tend of be more symmetric (normal law). This scale-dependence is the natural consequence of the Central Limit Theorem applied to HPE concentrations in the Earth crust. The importance of this effect is controlled by the distance of spatial auto-correlation of HPE concentrations, which may vary from one element to the other. Quantitative interpretations of airborne radiometric surveys are combined with different sources of information in many applications (geological mapping, mineral exploration, geothermal projects). Such applications must therefore carefully consider the scale transfer problem when integrating different sources of data for HPE concentrations. The relatively short distances of spatial auto-correlations (or the relatively large degree of heterogeneities of concentrations over short distances) of the three elements is a direct consequence of their geochemical behavior (incompatible elements for HPE, and immobility of Th and U in many contexts). This behavior may be tentatively extrapolated to other minor or trace elements with similar geochemical behavior. The existence of relationships between univariate and spatial statistics and geochemical behavior is a relatively unexplored area of research which will be explored in future studies.

References

Ahrens, L. H. (1954). The lognormal distribution of the elements (A fundamental law of geochemistry and its subsidiary). *Geochimica et Cosmochimica Acta*, *5*(2), 49–73. https://doi.org/10.1016/0016-7037(54)90040-X

Allegre, C. J., & Lewin, E. (1995). Scaling Laws and Geochemical Distributions. *Earth and Planetary Science Letters*, *132*(1–4), 1–13.

Baratoux, L., Metelka, V., Naba, S., Jessell, M. W., Grégoire, M., & Ganne, J. (2011). Juvenile Paleoproterozoic crust evolution during the Eburnean orogeny (~2.2-2.0Ga), western Burkina Faso. *Precambrian Research*, *191*(1–2), 18–45. https://doi.org/10.1016/j.precamres.2011.08.010

Bodorkos, S., Sandiford, M., Minty, B. R. S., & Blewett, R. S. (2004). A high-resolution, calibrated airborne radiometric dataset applied to the estimation of crustal heat production in the Archaean northern Pilbara Craton, Western Australia. *Precambrian Research*, *128*(1–2), 57–82. https://doi.org/10.1016/j.precamres.2003.08.008

Bourdon, B., Turner, S., Henderson, G. M., & Lundstrom, C. C. (2003). Introduction to U-series geochemistry. *Reviews in Mineralogy and Geochemistry*, *52*, 1–21. https://doi.org/10.2113/0520001

Bullock, M. A., & Moore, J. M. (2004). Aqueous alteration of Mars-analog rocks under an acidic atmosphere. *Geophysical Research Letters*, *31*(14), 2–5. https://doi.org/10.1029/2004GL019980

Carpentier, M., Weis, D., & Chauvel, C. (2013). Large U loss during weathering of upper continental crust: The sedimentary record. *Chemical Geology*, *340*, 91–104. https://doi.org/10.1016/j.chemgeo.2012.12.016

Champion, D. (2015). *OZCHEM national whole rock geochemistry dataset.* www.ga.gov.au/metadata-gateway/metadata/record/gcat 65464.

Chardon, D., Grimaud, J.-L., Beauvais, A., & Bamba, O. (2018). West African lateritic pediments: Landform-regolith evolution processes and mineral exploration pitfalls. *Earth-Science Reviews*, *179*, 124–146. https://doi.org/10.1016/j.earscirev.2018.02.009

Cuney, M. (2010). Evolution of Uranium Fractionation Processes through Time: Driving the Secular Variation of Uranium Deposit Types. *Economic Geology*, *105*(3), 553–569. https://doi.org/10.2113/gsecongeo.105.3.553

Dentith, M., & Mudge, S. T. (Eds.). (2014). Radiometric method. In *Geophysics for the mineral exploration geoscientist*. Cambridge: Cambridge University Press.

Dickson, B. L., & Scott, K, M. (1997). Interpretation of aerial gamma-ray surveys - adding the geochemical factors. *Journal of Australian Geology & Geophysics*.

Fall, M., Baratoux, D., Ndiaye, P. M., Jessell, M., & Baratoux, L. (2018). Multi-scale distribution of Potassium. Thorium and Uranium in Paleoproterozoic granites from eastern Senegal. *Journal of African Earth Sciences*, *148*, 30–51. https://doi.org/10.1016/j.jafrearsci.2018.03.026

Fall, M., Baratoux, D., Jessell, M., Ndiaye, P. M., Vanderhaeghe, O., Moyen, J. F., et al. (2020). The redistribution of thorium, uranium, potassium by magmatic and hydrothermal processes versus surface processes in the Saraya Batholith (Eastern Senegal): Insights from airborne radiometrics data and topographic roughness. *Journal of Geochemical Exploration*, 106633. https://doi.org/10.1016/j.gexplo.2020.106633

Gale, A., Dalton, C. A., Langmuir, C. H., Su, Y., & Schilling, J. G. (2013). The mean composition of ocean ridge basalts. *Geochemistry, Geophysics, Geosystems*, *14*(3), 489–518. https://doi.org/10.1029/2012GC004334

Goldfarb, R. J., André-Mayer, A. S., Jowitt, S. M., & Mudd, G. M. (2017). West Africa: The world's premier Paleoproterozoic gold province. *Economic Geology*, *112*(1), 123–143. https://doi.org/10.2113/econgeo.112.1.123

Grasty, R. L. (1987). *The design, construction, and application of airborne gamma-ray spectrometer calibration pads, Thailand*. Ottawa, Canada: Geological Survey of Canada.

Hein, K. A. A. (2016). West African mineral Atlas monograph. *Ore Geology Reviews*, *78*, 556–557. https://doi.org/10.1016/j.oregeorev.2016.04.001

Jessell, Mark W., & Liégeois, J.-P. (2015). 100 years of research on the West African Craton. *Journal of African Earth Sciences*, *112*, 377–381. https://doi.org/10.1016/j.jafrearsci.2015.10.008

Jessell, Mark W., Cawood, P. A., & Miller, J. M. (2016). Craton to Regional-scale analysis of the Birimian of West Africa. *Precambrian Research*, *274*, 1–2. https://doi.org/10.1016/j.precamres.2015.12.014

Jessell, M.W. et al. (2018). *Module 4.2 Physico-chemical properties of the regolith* (West African Exploration Initiative - Stage 3 No. P934B) (p. 852). Amira International.

Jones, M. C., Marron, J. S., & Sheather, S. J. (1996). A Brief Survey of Bandwidth Selection for Density Estimation Stable URL : http://www.jstor.org/stable/2291420 Linked references are available on JSTOR for this article : A Brief Survey of Bandwidth Selection for Density Estimation. *Journal of the American Statistical Association*, *91*(433), 401–407.

Kirkland, C. L., Smithies, R. H., Taylor, R. J. M., Evans, N., & McDonald, B. (2015). Zircon Th/U ratios in magmatic environs. *Lithos*, *212–215*, 397–414. https://doi.org/10.1016/j.lithos.2014.11.021

Kranendonk, M. J. V., Hickman, A. H., Smithies, R. H., Nelson, D. R., & Pike, G. (2002). Geology and Tectonic Evolution of the Archean North Pilbara Terrain,Pilbara Craton,

Western Australia. *Economic Geology*, *97*(4), 695–732.
https://doi.org/10.2113/gsecongeo.97.4.695

Langmuir, C. H., Hanson, G. N., & O'Hara, M. J. (1980). An Evaluation of Major Element Heterogeneity in the Mantle Sources of Basalts [and Discussion]. *Philosophical Transactions of the Royal Society A: Mathematical, Physical and Engineering Sciences*, *297*(1431), 383–407. https://doi.org/10.1098/rsta.1980.0223

Metelka, V., Baratoux, L., Naba, S., & Jessell, M. W. (2011). A geophysically constrained litho-structural analysis of the Eburnean greenstone belts and associated granitoid domains, Burkina Faso, West Africa. *Precambrian Research*, *190*(1–4), 48–69. https://doi.org/10.1016/j.precamres.2011.08.002

Metelka, V., Baratoux, L., Jessell, M. W., Barth, A., Ježek, J., & Naba, S. (2018). Automated regolith landform mapping using airborne geophysics and remote sensing data, Burkina Faso, West Africa. *Remote Sensing of Environment*, *204*, 964–978. https://doi.org/10.1016/j.rse.2017.08.004

Milési, J.-P., Ledru, P., Feybesse, J.-L., Dommanget, A., & Marcoux, E. (1992). Early proterozoic ore deposits and tectonics of the Birimian orogenic belt, West Africa. *Precambrian Research*, *58*(1–4), 305–344. https://doi.org/10.1016/0301-9268(92)90123-6

Minty, B.; Richardson, M., Wilford, J. (2008). *New radiometric map of australia - http://www.ga.gov.au/ausgeonews/ausgeonews200812/radiometrics.jsp*.

Mohamud, A. H., Cózar, J. S., Rodrigo-Naharro, J., & Pérez del Villar, L. (2015). Distribution of U and Th in an Iberian U-fertile granitic complex (NW, Spain): Airborne-radiometry, chemical and statistical approaches. *Journal of Geochemical Exploration*, *148*, 40–55. https://doi.org/10.1016/j.gexplo.2014.07.022

Moyen, Jean-François, Cuney, M., Baratoux, D., & Sardini, P. (In press). Multi-scale spatial distribution of K, Th and U in an Archean potassic granite: a case study from the Heerenveen batholiith, Baberton Granite-Greenstone Terrain, South Africa. *South African Journal of Geology*.

Moyen, J-F., Cuney, M., Baratoux, D., Sardini, P., & Carrouée, S. (2021). Multi-scale spatial distribution of K, Th and U in an Archaean potassic granite: a case study from the Heerenveen batholith, Barberton Granite-Greenstone Terrain, South Africa. *South African Journal of Geology*. https://doi.org/10.25131/sajg.124.0005

Phaneuf, C., & Mareschal, J. C. (2014). Estimating concentrations of heat producing elements in the crust near the Sudbury Neutrino Observatory, Ontario, Canada. *Tectonophysics*, *622*, 135–144. https://doi.org/10.1016/j.tecto.2014.03.001

Rosenblatt, M. (1956). Remarks on some nonparametric estimates of a density function. *The Annals of Mathematical Statistics*, *27*(3), 832–837.

Rubatto, D. (2002). Zircon trace element geochemistry: partitioning with garnet and the link between U–Pb ages and metamorphism. *Chemical Geology*, *184*(1–2), 123–138. https://doi.org/10.1016/S0009-2541(01)00355-2

Tartèse, R., Boulvais, P., Poujol, M., & Vigneresse, J. L. (2011). Granite petrogenesis revealed by combined gravimetric and radiometric imaging. *Tectonophysics*, *501*(1–4), 98–103. https://doi.org/10.1016/j.tecto.2011.02.003

De Wijs, H. J. (1953). DeWijs1953.pdf. *Geol. Mijnbouw*, *15*, 12–24.

Wilford, J. (2012). A weathering intensity index for the Australian continent using airborne gamma-ray spectrometry and digital terrain analysis. *Geoderma*, *183–184*, 124–142. https://doi.org/10.1016/j.geoderma.2010.12.022

Wilford, J. R., Searle, R., Thomas, M., Pagendam, D., & Grundy, M. J. (2016). A regolith depth map of the Australian continent. *Geoderma*, *266*, 1–13. https://doi.org/10.1016/j.geoderma.2015.11.033

Williams, I. S., Buick, I. S., & Cartwright, I. (2004). An extended episode of early Mesoproterozoic metamorphic fluid flow in the Reynolds Range, central Australia*. *Journal of Metamorphic Geology*, *14*(1), 29–47. https://doi.org/10.1111/j.1525-1314.1996.00029.x

Xhixha, M. K., Albèri, M., Baldoncini, M., Bezzon, G. P., Buso, G. P., Callegari, I., et al. (2016). Uranium distribution in the Variscan Basement of Northeastern Sardinia. *Journal of Maps*, *12*(5), 1029–1036. https://doi.org/10.1080/17445647.2015.1115784

Youssef, M. A. S. (2016). Estimating and interpretation of radioactive heat production using airborne gamma-ray survey data of Gabal Arrubushi area, Central Eastern Desert, Egypt. *Journal of African Earth Sciences*, *114*, 67–73. https://doi.org/10.1016/j.jafrearsci.2015.10.022